

# **Design of An Active element-based Class-J Power Amplifier for 5G Wireless Communication Applications**

**By**

**Nagisetty Sridhar**

Faculty of Engineering, Multimedia University, Cyberjaya, Selangor, Malaysia

Email: [sridharnagisetty@gmail.com](mailto:sridharnagisetty@gmail.com)

**C Senthilpari**

Faculty of Engineering, Multimedia University, Cyberjaya, Selangor, Malaysia

**Mardeni R**

Faculty of Engineering, Multimedia University, Cyberjaya, Selangor, Malaysia

**Wong Hin Yong**

Faculty of Engineering, Multimedia University, Cyberjaya, Selangor, Malaysia

## **Abstract**

This paper presents the analysis and design of an active element-based class-J Power Amplifier (PA). A proper PA needs to be designed to achieve the required power output over a bandwidth (BW) that supports the emerging 5G applications without sacrificing linearity. Among different PAs, class-J mode PA will be more suitable for linear and broadband applications. Therefore, a class-J PA design that operates at 5GHz (i.e., sub-6GHz 5G frequency band) with an active element-based approach using Silterra 130nm CMOS process technology to estimate its feasibility for integration without compromising on the performance is described in this paper. The simulation results show that the saturated power output ( $P_{sat}$ ) of 27dBm with a maximum value of 13.73dB power gain and power output at 1dB compression point ( $P_{1dB}$ ) of 26.2dBm are obtained with a BW of approximately 500 MHz by supplying the PA with 5V to deliver into 50  $\Omega$  load. The PA's layout with the estimated chip size of (13.8X20.0)  $\mu\text{m}^2$  reveals its feasibility for the integration.

**Keywords:** 5G, Sub-6GHz, Class-J, Power Amplifier, OMN

## **Introduction**

The most key building block of emerging 5G [1-3] wireless communication systems is PA, as its performance has a crucial impact on the overall system's energy consumption and BW enhancement. Among various PA modes reported in the literature [4-12], the class-J PA proposed by Steve C. Cripps in 2006 [11] has proved its potentiality and suitability for linear and broadband applications. Because of class-J PA's good wideband and linear performance it has been analysed and designed by many research scholars for different applications [13-17]. However, to achieve the required power output over desired BW of 5G applications, this class-J PA design with a tuneable inductor or capacitor-based dynamic Output Matching Network (OMN) is preferred [18]. Because, transistor's non-linear parasitic parameters that operates in class-J PA, changes the value its optimum impedance under different frequencies which directly varies the impedance value of OMN. Moreover, the emerging 5G technology need to support the higher data rates in applications such as the 5G smart meter/grid [19]. Therefore, proper OMN is becoming crucial to make this well-established class-J PA suitable for such 5G applications. In this work, the optimum impedance needed for class-J PA is calculated using

extensive waveform engineering instead of load-pull simulations, then to match this optimum impedance with the load resistance ( $R_L$ ), an OMN with  $\pi$ -type structure is designed with an idea to replace its passive inductor with tuneable active inductor [20]. Finally, to check the PA circuit's feasibility for integration via its chip size estimation, all its passive components are replaced by active elements without affecting its performance. The class-J PA's theory is analysed in Section II. In Section-III the analysis and calculation of optimum impedance is described. The  $\pi$ -type OMN design to achieve class-J operation is elaborated in Section-IV. In Section-V the simulation results of the designed PA and their comparison with recent similar PA designs are discussed. In Section-VI this work's summary is briefed as conclusion.

## Theory and Analysis of Class-J Pa

Based on the class-J PA's theory, with the class-B biasing point the transistor's drain current ( $I_D$ ) is expressed as shown in equation (1).

$$I_D | j(\theta) = \frac{I_{max}}{\pi} + \frac{I_{max}}{2 \cos(\theta)} + \frac{2I_{max}}{3\pi \cos(2\theta)} \quad (1)$$

$I_{max}$  is the transistor's maximum ID.

The voltage at the drain of the transistor ( $V_{DS}$ ) expressed in equation (2) is obtained by presenting it with an inductive fundamental load and a capacitive second harmonic load.

$$V_{DS} | j = V_{th} + (V_{DD} - V_{th})(1 - \cos \theta)(1 + \alpha \sin \theta) \quad (2)$$

$V_{DD}$  and  $V_{th}$  are the transistor's supply and threshold voltages.

The theoretical optimum impedances required for class-J operation mode are extracted from equations (1) & (2), can be expressed as shown in equations (3) & (4).

$$Z_{f0} = \frac{(V_{DD} - V_{th})(1 + j\alpha)}{I_{max}/2} = R_{opt} + j\alpha R_{opt} \quad (3)$$

$$Z_{2f0} = -\frac{(V_{DD} - V_{th})j\alpha}{2\left(\frac{2I_{max}}{3\pi}\right)} = -\frac{j3\pi}{8} \alpha R_{opt} \quad (4)$$

Equation (5) represents the transistor's optimum resistance

$$R_{opt} = 2(V_{DD} - V_{th}) \div I_{max} \quad (5)$$

By presenting these  $Z_{f0}$  &  $Z_{2f0}$  to the transistor a boost in the drain voltage ( $V_{DS}$ ) with some phase shift that reduces overlap between  $V_{DS}$  and  $I_D$ , can be observed as shown in Figure 1, making the class-J PA more efficient.

In addition, due to its non-switching operation mode this class-J PA's linearity will be same as class-B or AB PAs, although the  $V_{DS}$  and  $I_D$  waveforms in Figure 1 resemble the switching mode PA's waveforms. This class-J PA will be more suitable for wideband applications as it will not use any harmonic traps like class-B PA.

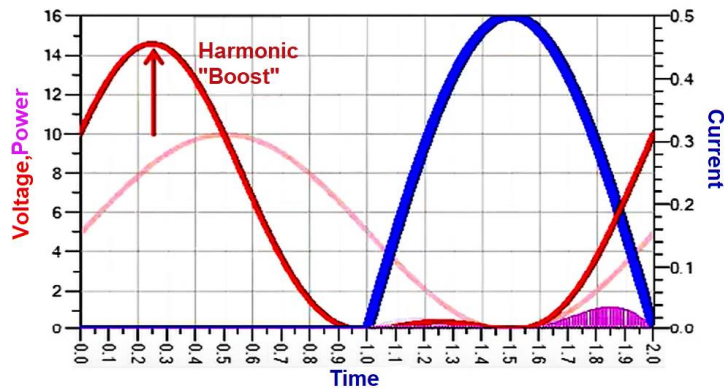


Figure 1. The  $V_{DS}$  and  $I_D$  of class-J PA's transistor

### Optimum Impedance Analysis

The values of optimum impedances ( $Z_{f0}$  &  $Z_{2f0}$ ) required for class-J PA operation are theoretically calculated from the  $V_{DS}$  and  $I_D$  expressions as shown in equations (3) & (4) in terms of  $R_{opt}$ . But in practice, these optimum impedance values will deviate from their theoretical values because of the transistor's non-linear capacitance variation with frequency and power output. Therefore, generally, these practical optimum impedance values can be determined with the help of load-pull simulations at different frequencies and power outputs.

There is no possibility to perform load-pull simulations for the PA design in the Mentor Graphics (MG) EDA tool used, therefore a reference  $R_{opt}$  value has been initially chosen. To obtain this reference  $R_{opt}$  value, the aspect ratio of the selected transistor is altered accordingly, because this  $R_{opt}$  value depends on its transistor's maximum drain current ( $I_{max}$ ), which can be changed by its (W/L) ratio and the biasing voltages.

Therefore, in this work, a 130nm Silterra nm\_hp transistor (M1) has been chosen to get the reference  $R_{opt}$  value of  $4.3 \Omega$ . To calculate the theoretical value of  $I_{max}$  corresponding to the reference  $R_{opt}$  value using equation (5), the  $V_{DD}$  and  $V_{th}$  values must be known. The value of  $V_{DD}$  has been chosen as 5V to allow for the maximum swing across the selected transistor M1. The  $V_{th}$  value of the transistor M1 is extracted from its transconductance (gm). The value of gm is obtained by differentiating the  $I_D$  concerning  $V_{GS}$  (i.e.,  $dI_D/dV_{GS}$ ), and then this gm value is differentiated concerning  $V_{GS}$  (i.e.,  $dgm/dV_{GS}$ ) with the use of EZ waveform calculator utility of the EDA tool to extract the  $V_{th}$  value. The  $V_{GS}$  value where the derivative of gm with respect to  $V_{GS}$  is maximum is taken as the transistor's  $V_{th}$  value (i.e.,  $V_{th} \cong 0.5V$ ), as shown in Figure 2.

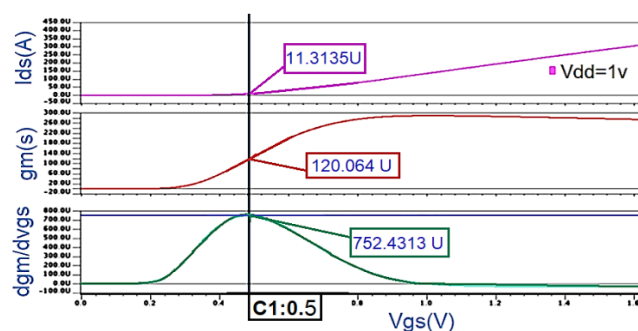
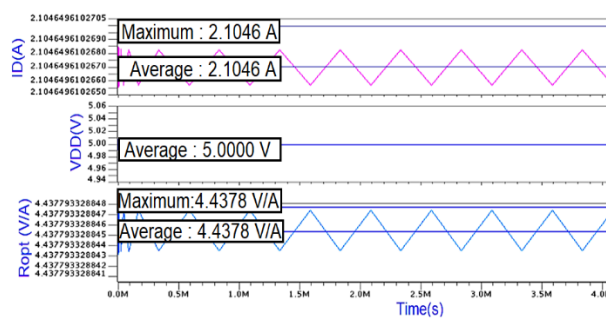


Figure 2.  $V_{th}$  value of nm-hp transistor

With these  $V_{DD}$  and  $V_{th}$  values, the theoretical  $I_{max}$  value calculated using equation (5) is 2.1A for corresponding reference  $R_{opt}$  value 4.3  $\Omega$ , and the theoretical optimum impedance values are obtained by substituting this  $R_{opt}$  value in equations (3) & (4).

To validate this theoretical optimum impedance value, the width (W) of the transistor (M1) is altered as (2x5 $\mu$ m) and is supplied with the bias voltages of  $V_{DD} = 5V$ ,  $V_{GS} \cong V_{th} \cong 0.5V$ . Corresponding to these bias voltages and transistor's size, the  $I_{max}$  value of 2.1A is obtained, leading to a  $R_{opt}$  value of approximately 4.5  $\Omega$ . This  $R_{opt}$  value is calculated with the help of EZ waveform calculator utility, as shown in Figure 3, is almost equal to its theoretical value.



**Figure 3.**  $R_{opt}$  obtained from EZ waveform calculator

As another approach, the transistor (M1)'s  $R_{opt}$  value can be determined by calculating its output impedance ( $Z_{out}$ ) in terms of S-parameters with the help of .extract and .defwave commands in the command window by conducting SST analysis at 5GHz frequency as shown in Figure 4.

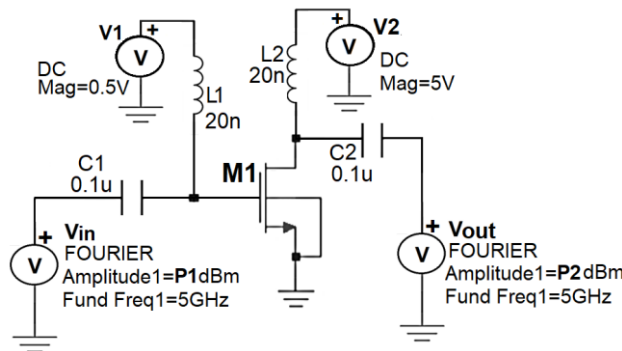


**Figure 4.** Extraction  $Z_{out}$  of the transistor (M1) from S-Parameters at 5GHz frequency

The class-J PA mode operation of the transistor can be achieved by matching its determined  $R_{opt}$  value of optimum impedances ( $Z_{f0}$  &  $Z_{2f0}$ ) with the load/output port resistance ( $R_L$ ) using a proper OMN design.

### 1. Design of $\Pi$ -Type OMN

A proper OMN design is the key to achieving class-J PA operation. Generally, the class-J PA's wideband operation can be achieved using different matching methods such as lumped passive element-based L,  $\pi$ , T-type networks or transmission lines based distributed networks. However, the transmission line based distributed OMN design may occupy a larger area which leads to an increase in the cost of integration, whereas the passive lumped-element based higher-order OMN design with a minimum of two inductors may reduce the power output and

efficiency due to the integrated inductor's losses used while implementing the PA circuit.

Therefore, initially the OMN using passive element-based  $\pi$ -structure with 2 capacitors and 1 inductor, as shown in Figure 5, has been chosen with an idea to replace its lumped inductor with an active inductor after achieving the PA's desired performance metrics.

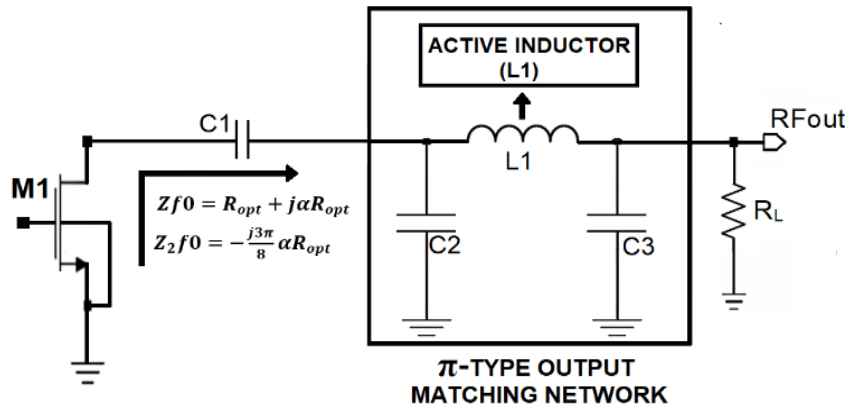


*Figure 5.  $\pi$ -type OMN design for class-J PA*

As the class-J PA of this work is planned to design at a centre frequency of 5GHz (i.e., sub-6GHz 5G frequency), its desired BW can be obtained by designing the OMN in terms of its Quality factor that will be represented as ( $Q=f/BW$ ). Therefore, this  $\pi$ -type OMN with two back-to-back connected L-sections is designed by choosing a Q value of 10 to achieve desired BW of approximately 500MHz to make the PA appealing for wideband 5G applications.

## Simulation Results And Discussion

The designed PA's performance with  $\pi$ -type OMN is validated by performing its schematic circuit simulations using the MG EDA tool. To achieve the class-J PA operation, the transistor (M1)'s drain is biased with voltage  $V_{DD} = 5V$ , the gate is biased with voltage  $V_{GS} \cong V_{th} \cong 0.5V$  (i.e., class-B bias point) and stabilized across desired frequency range using a simple RC circuit. The class-J PA's schematic circuit with its  $\pi$ -type OMN is shown in Figure 6.

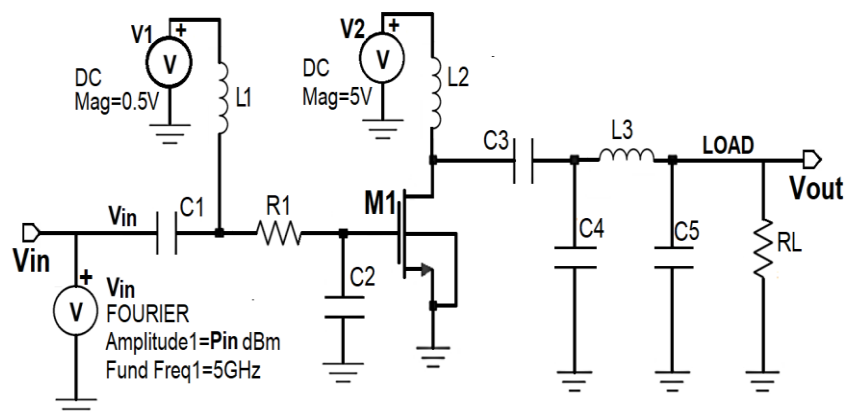


*Figure 6. Schematic class-J PA circuit with*

$$(R_{opt} \cong \text{Ref } R_{opt}) \text{ and } (R_{opt} \cong Z_{out})$$

The component values of schematic class-J PA circuit whose OMNs designed corresponding to value of  $R_{opt}$  calculated using EZ waveform calculator (i.e.,  $R_{opt} \cong Ref R_{opt}$ ) and  $R_{opt}$  value equal  $Z_{out}$  of the transistor (M1) which is obtained in terms of S-parameters (i.e.,  $R_{opt} \cong Z_{out}$ ) are shown in the Table-1.

**Table -1: Component values of Figure 6**

Components	Values corresponding to OMNs with	
	$(R_{opt} \cong Ref R_{opt})$	$(R_{opt} \cong Z_{out})$
C1=C3	0.1uF	0.1uF
C2	5pF	5pF
C4	5.2pF	16.5pF
C5	2.6pF	6.4pF
L1=L2	20nH	20nH
L3	0.45nH	0.2nH
R1	10Ω	10Ω
RL	50Ω	50Ω

Then, this designed class-J PA is supplied with 1-Tone Continuous Wave (CW) RF input signal with a centre frequency of 5GHz to evaluate its performance. The important performance parameter waveforms of the simulated PA are obtained by typing their mathematical expressions in command window while performing SST analysis corresponding to the power input (Pin) sweep of Fourier RF input source as shown in Figure 7. It is noticed that the PA delivers 11 dB maximum power gain and 26 dBm  $P_{sat}$  value.

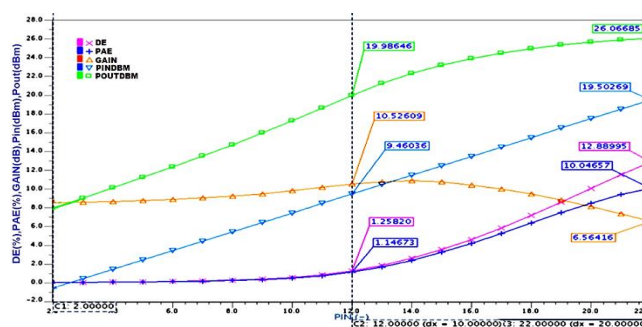


**Figure 7. The class-J PA's performance parameters with  $(R_{opt} \cong Ref R_{opt})$**

Similarly, the class-J PA's performance parameters with its  $\pi$ -type OMN designed corresponding to the,  $R_{opt}$  value equal  $Z_{out}$  of the transistor (M1) which is obtained in terms of S-parameters (i.e.,  $R_{opt} \cong Z_{out}$ ) are shown in Figure 8.

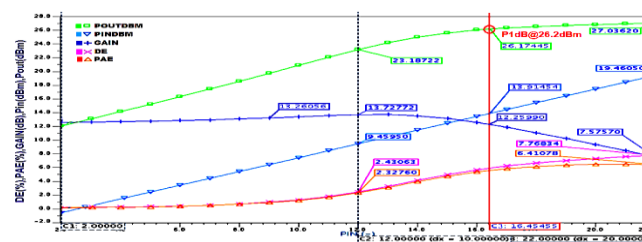


**Figure 8. The class-J PA's performance parameters with  $(R_{opt} \cong Z_{out})$**

It is noticed that when this PA is supplied with the same 1-Tone CW RF input signal at 5GHz centre frequency, the PA delivers a  $P_{sat}$  value of 27dBm and 13.73dB maximum power

gain for a BW approximately 500 MHz corresponding to the Q factor value chosen. In addition, the PA's linearity is measured using a 1dB compression point (P1dB). The Pout delivered at P1dB is 26.2dBm which is almost equal to  $P_{sat}$ , it represents that the PA is exhibiting good linearity.

Post validation of PA's performance parameters its layout is designed for the chip size estimation. As this PA is initially designed using lumped passive components, not only the lumped inductor of  $\pi$ -type OMN, all other passive components of the PA also replaced by active elements (transistors) as shown in Figure 9.

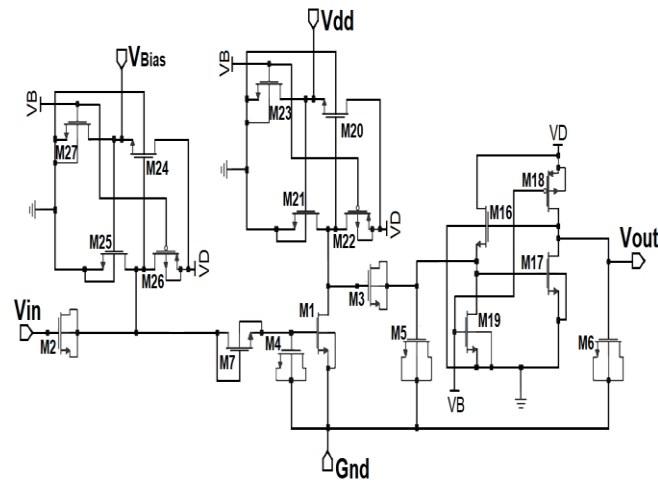


**Figure 9.** Active element-based schematic circuit for layout design of class-J PA

The designed class-J PA layout simulation has been carried out using MG EDA tool. The optimization and arrangement of transistors was made to reduce its chip area. The estimated chip layout size of this active element-based class-J PA is  $(13.8 \times 20.0) \mu\text{m}^2$  as shown in Figure 10.

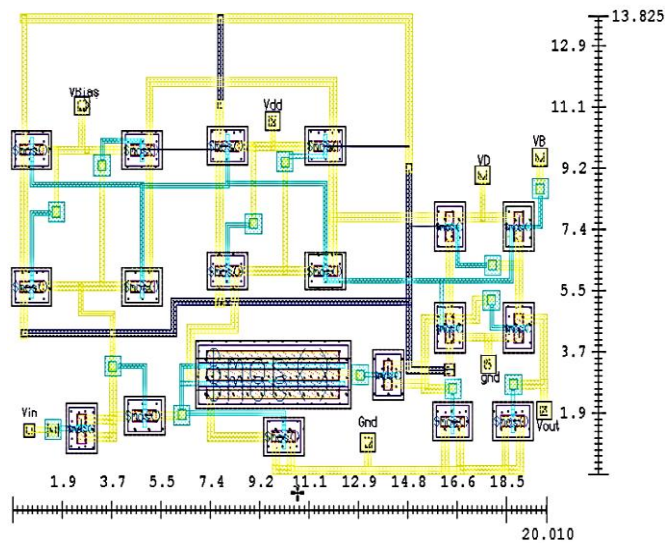


**Figure 10.** The core layout of class-J PA  $(13.8 \times 20.0) \mu\text{m}^2$

This class-J PA's performance parameter comparison with similar recently published PAs is shown in Table-2.

**Table-2.** class-J PA's Performance comparison

Reference	This work	[24] 2021	[23] 2020	[22] 2018	[21] 2017
Technology	CMOS	CMOS	GaN	GaN	CMOS
Class	J	J	J	J	J
Stage	Single	Two	Single	Single	Two
Frequency[GHz]	5	9.5	3.2	3	28
BW [GHz]	4.8-5.3	8.7-11.8	2.5-3.8	2.5-3.5	22-34
P1dB[dBm]	26.2	18	-	-	-
Psat [dBm]	27	20	42	40	16.2
Max Gain [dB]	13.73	15	13.3	10	15

The class-J PA designs shown in Table-2 were used different technologies and frequencies, hence their comparison is bit difficult. Irrespective of the difficulty in comparison, it is worth noting that a 28GHz two-stage class-J PA design using 28nm CMOS technology reported in [21] delivers a 15dB power gain and 16.2 dBm  $P_{sat}$ , whereas our single-stage class-J PA delivers 13.73 dB maximum power gain and 27 dBm  $P_{sat}$ . A class-J PA design with high power GaN transistor in [22] delivers 10 dB maximum power gain and 40 dBm  $P_{sat}$ , whereas our class-J PA with 130nm Silterra transistor delivers 13.73 dB maximum power gain with 27dBm  $P_{sat}$  along with 26.2 dBm Pout at P1dB which is almost equal to  $P_{sat}$  represents its good linearity. A class-J PA with a novel OMN synthesis technique for presented in [23] delivers a  $P_{sat}$  of 42dBm with 13dB power gain and good efficiency over broadband using 10W GaN transistor, although our PA design uses a 130nm Silterra transistor it delivers a 13.73 dB maximum power gain. A 130nm CMOS class-J PA that delivers 20.2 dBm  $P_{sat}$  with 15 dB maximum power gain using two-stage structure is reported in [24], however our PA design 13.73dB maximum power gain using single-stage. Although, our class-J PA design delivers the good power gain with linearity and exhibits its feasibility for integration, the remaining PA's performance metrics like BW and efficiency can be further improved to implement it in emerging wideband 5G applications.

## Conclusion

Initially in this paper, the selected transistor's optimum impedance ( $R_{opt}$ ) value is analysed and determined using waveform engineering and by calculating the  $Z_{out}$  of the transistor from its S-parameters, which is needed to achieve class-J PA operation. Finally, a class-J PA with  $\pi$ -type OMN that matches the determined optimum impedance with a load impedance of output port is designed, which delivers a  $P_{sat}$  of 27dBm with a maximum value of 13.73dB power gain over a BW of approximately 500MHz. The P1dB of PA is almost nearer to its  $P_{sat}$  value, revealing that it can provide good linearity. In addition, this active-element-based class-J PA's layout reveals that it is feasible for integration. However, the enhancement work of this PA's other performance metrics like BW and efficiency is in progress to improve its suitability for (sub- 6GHz) 5G wideband applications.

## Acknowledgment

We sincerely thank Ministry of Higher Education (MOHE), Malaysia for supporting

this research by funding through FRGSMMUE/190075 and Multimedia university for providing this opportunity.

**2. Competing Interests**

No competing interests were disclosed.

**3. Data availability**

No data is associated with this manuscript.

**4. Grant Information**

This research work is funded by The Ministry of Higher Education, Malaysia under the FRGS grants.

## References

- Dahiya, Menal. (2017). "Need and Advantages of 5G wireless Communication Systems". *International Journal of Advanced Research in Computer Science & Management Studies*. 5. 48-51.
- D. Y. C. Lie, J. C. Mayeda, Y. Li, J. Lopez, "A Review of 5G Power Amplifier Design at cm-Wave and mm-Wave Frequencies", *Wireless Communications and Mobile Computing*, vol. 2018, Article ID 6793814, 16 pages, 2018. <https://doi.org/10.1155/2018/6793814>  
<https://www.digi.com/blog/post/5G-applications-and-use-cases>
- S. A. Z. Murad, M. F. Ahamd, M. M. Shahimin, R. C. Ismail, K. L. Cheng, and R. Sapawi, "High-efficiency CMOS Class E power amplifier using 0.13  $\mu\text{m}$  technology," 2012 IEEE Symposium on Wireless Technology and Applications (ISWTA), 2012, pp. 85-88, DOI: 10.1109/ISWTA.2012.6373883.
- Sahu, Shridhar & Deshmukh, Amol. (2013). Design of High-Efficiency Two-Stage Power Amplifier in 0.13 $\mu\text{M}$  RF CMOS Technology for 2.4GHZ WLAN Application. *International Journal of VLSI Design & Communication Systems*. 4. 31-40. DOI 10.5121/vlsic.2013.4404.
- Yi-Hsin Chen, K. Kao, Chun-Yen Chao, and K. Lin, "A 24 GHz CMOS power amplifier with successive IM2 feed-forward IMD3 cancellation," 2015 IEEE MTT-S International Microwave Symposium, 2015, pp. 1-4, DOI: 10.1109/MWSYM.2015.7166914.
- Kazuaki Junichiro, Shinichi hori, Tomoya kaneko, "High Efficiency Power Amplifiers for Mobile Base Stations: Recent Trends and Future Prospects for 5G", *IEICE Transactions on Fundamentals of Electronics, Communications and Computer Sciences*, 2018, Volume E101.A, Issue 2, Pages 374-384, Released February 01, 2018, Online ISSN 1745-1337, Print ISSN 0916-8508, <https://doi.org/10.1587/transfun.E101.A.374>
- P. Reynaert, Y. Cao, M. Vigilante and P. Indirayanti, "Doherty techniques for 5G RF and mm-wave power amplifiers," 2016 International Symposium on VLSI Technology, Systems and Application (VLSI-TSA), 2016, pp. 1-2, DOI: 10.1109/VLSI-TSA.2016.7480475.
- P. M. Asbeck, "Will Doherty continue to rule for 5G?" 2016 IEEE MTT-S International Microwave Symposium (IMS), 2016, pp. 1-4, DOI: 10.1109/MWSYM.2016.7540208.

- J. A. Jayamon, J. F. Buckwalter and P. M. Asbeck, "28 GHz >250 mW CMOS Power Amplifier Using Multigate-Cell Design," 2015 IEEE Compound Semiconductor Integrated Circuit Symposium (CSICS), 2015, pp. 1-4, DOI: 10.1109/CSICS.2015.7314460.
- S. C. Cripps, RF Power Amplifiers for Wireless Communications, 2nd ed. Boston, MA, Artech, 2006.
- P. Wright, J. Lees, J. Benedikt, P. J. Tasker, and S. C. Cripps, "A methodology for realizing high-efficiency class-J in a linear and broadband PA" IEEE Trans. Microwave Theory Tech., vol. 57, no. 12, pp.3196–3204, Dec. 2009
- S. Rezaei, L. Belostotski, F. M. Ghannouchi, and P. Alfaki, "Integrated Design of a Class-J Power Amplifier" in IEEE Transactions on Microwave Theory and Techniques, vol. 61, no. 4, pp. 1639-1648, April 2013, DOI: 10.1109/TMTT.2013.2247618.
- Y. Dong, L. Mao, and S. Xie, "Fully Integrated Class-J Power Amplifier in Standard CMOS Technology," in IEEE Microwave and Wireless Components Letters, vol. 27, no. 1, pp. 64-66, Jan. 2017, DOI: 10.1109/LMWC.2016.2630920.
- A. Alizadeh, M. Frounchi and A. Medi, "Waveform Engineering at Gate Node of Class-J Power Amplifiers," in IEEE Transactions on Microwave Theory and Techniques, vol. 65, no. 7, pp. 2409-2417, July 2017 DOI: 10.1109/TMTT.2017.2651814.
- A. Alizadeh and A. Medi, "Investigation of a Class-J Mode Power Amplifier in Presence of a Second-Harmonic Voltage at the Gate Node of the Transistor," in IEEE Transactions on Microwave Theory and Techniques, vol. 65, no. 8, pp. 3024-3033, Aug. 2017, DOI: 10.1109/TMTT.2017.2666145.
- A. Alizadeh, M. Yaghoobi and A. Medi, "Class-J2 Power Amplifiers," in IEEE Transactions on Circuits and Systems I: Regular Papers, vol. 64, no. 8, pp. 1989-2002, Aug. 2017, DOI: 10.1109/TCSI.2017.2683067.
- W. Gao, Y. Luo, C. Shen and R. Lei, "Design of Class-J Power Amplifier with Dynamic Matching Network for 5G Frequency Band," 2020 IEEE 20th International Conference on Communication Technology (ICCT), 2020, pp. 472-475, DOI: 10.1109/ICCT50939.2020.9295827.
- Y. K. Hiew, N. M. Aripin, S. Jayavalan, and N. M. Din, "Spectrum band for smart grid implementation in Malaysia," 2013 IEEE Student Conference on Research and Development, 2013, pp. 26-30, DOI: 10.1109/SCORED.2013.7002534
- Alireza Saberhari, Saman Ziabakhsh, Herminio Martinez, Eduard Alarcón, "Active inductor-based tunable impedance matching network for RF power amplifier application", Integration, Volume 52,2016, Pages 301-308, ISSN 0167-9260, <https://doi.org/10.1016/j.vlsi.2015.07.013>.
- T. Hanna, N. Deltimple and S. Frégonèse, "A class-J power amplifier for 5G applications in 28nm CMOS FD-SOI technology," 2017 30th Symposium on Integrated Circuits and Systems Design (SBCCI), 2017, pp. 110-113.
- E. C. Tubitak, O. Palamutcuogullan, O. K. Tubitak, B. S. Yarman and M. Yazgi, "High Efficiency Wideband Power Amplifier with Class-J Configuration," 2018 18th

Mediterranean Microwave Symposium (MMS), 2018, pp. 394-397, doi: 10.1109/MMS.2018.8612039.

Zeng, M, Chen, S, Wang, W, Cai, J, Cao, W, Zhou, XY, Chan, WS & Wang, G 2020, 'A novel direct matching network synthesis technique and its application to broadband class-J power amplifier', International Journal of RF and Microwave Computer-Aided Engineering, vol. 30, no. 11, e22390. <https://doi.org/10.1002/mmce.22390>

P. Zhang et al., "An X-Band Broadband High-Efficiency Power Amplifier with Class-J Mode Matching Network," 2021 International Conference on Microwave and Millimeter Wave Technology (ICMMT), 2021, pp. 1-3, DOI: 10.1109/ICMMT52847.2021.9617933.